Synapse Compression for Event-Based Convolutional-Neural-Network Accelerators

Lennart Bamberg*, Arash Pourtaherian†, Luc Waeijen†, Anupam Chahar*, and Orlando Moreira†

*At the time of writing with GrAI Matter Labs: bamberg@uni-bremen.de, aschahar@gmail.com
†GrAI Matter Labs: {apourtaherian, lwaeijen, omoreira}@graimatterlabs.ai

arXiv:2112.07019v3 [cs.AR] 24 Jan 2023

Abstract—Manufacturing-viable neuromorphic chips require novel compute architectures to achieve the massively parallel and efficient information processing the brain supports so effortlessly. The most promising architectures for that are spiking/event-based, which enables massive parallelism at low complexity. However, the large memory requirements for synaptic connectivity are a showstopper for the execution of modern convolutional neural networks (CNNs) on massively parallel, event-based architectures. The present work overcomes this roadblock by contributing a lightweight hardware scheme to compress the synaptic memory requirements by several thousand times—enabling the execution of complex CNNs on a single chip of small form factor. A silicon implementation in a 12-nm technology shows that the technique achieves a total memory-footprint reduction of up to $374 \times$ compared to the best previously published technique at a negligible area overhead.

Index Terms—CNN, hardware accelerator, compression, sparsity, neuromorphic, spiking, dataflow, event-based, near-memory compute

1 INTRODUCTION

Convolutional neural networks (CNNs) achieve state-of-the-art computer-vision performance. Neural networks are not only more accurate but also easier to develop than hand-crafted techniques. Thereby, they enable a plethora of applications, opening new markets for digital systems.

One of the challenges CNNs pose is their large computational complexity and the massive parameter count (e.g., *ResNet50* requires over $23\,\text{M}$ parameters and $4\,\text{GFLOPS/frame}$ [1]). Therefore, CNN inference is relatively slow and power-hungry on traditional general-purpose compute architectures, as it requires a large number of expensive DRAM accesses and arithmetic operations. Thus, high frame-rate and yet low-power CNN inference is challenging on constrained edge devices. Consequently, accelerators for efficient CNN inference at the edge are one of the largest research topics in industry and academia today.

Some of the most promising processor architectures for efficient CNN inference are dataflow/event-based with a self-contained memory organization [2]–[4]. The neuromorphic dataflow model of computation, where execution is triggered on the arrival of data exchanged through events rather than by a sequential program, enables scaling to massive core counts at low complexity. Moreover, dataflow cores are typically lighter in hardware implementation than more traditional *von-Neumann* processors.

Table 1
Neuron and synapse count of CNNs and the maximum capabilities of event-based architectures from major semiconductor companies.

	CNNs			Architecture	
	PilotNet [10]	*MobileNet* [9]	*ResNet50* [1]	*IBM* [4]	*Intel* [2], [8]
Neurons	0.2 M	4.4 M	9.4 M	1.1 M	1.1 M
Synapses	27 M	0.5 B	3.8 B	0.3 B	0.1 B

Another advantage of event-based systems is that they can exploit the large degrees of activation/firing sparsity in modern deep neural networks. This is especially true for leak-integrate-and-fire (LIF) or sigma-delta neuron models, which exploit temporal correlation in the input and the feature maps to increase sparsity [3], [5]. Thus, event-based processing delivers massive compute performance at low power consumption and area.

A self-contained memory architecture overcomes DRAM access bottlenecks, as all parameters required during execution are stored in local on-chip memories, distributed over the cores. This avoids slow and power-hungry DRAM accesses entirely. The need for no external DRAM makes the system not only more efficient power and performance wise, but also cheaper and smaller. This further enhances the suitability of event-based systems for embedded applications.

Due to these vast promises, a range of event-based and self-contained architectures was designed by academia [6], [7], and global semiconductor companies like *Intel* and *IBM* [2]–[4], [8]. However, many of the existing chips only allow a limited neuron count and hence do not support the inference of modern sophisticated CNNs (e.g., *ResNet* [1] or *MobileNet* [9]). A fundamental problem is the memory requirement for synapses, i.e., the weighted connections between the neurons. Published event-based architectures, store the synapses in (hierarchical) look-up tables (LUTs), resulting in memory requirements that scale with the total neuron count. This leads to high memory requirements for neural networks with a large neuron and synapse count. Consequently, architectures like *Intel*'s *Loihi* and *IBM*'s *TrueNorth* are not capable to execute modern, sophisticated CNNs as shown in Table 1. Sophisticated CNN models are still out of reach for existing event-based architectures, limiting their usability today.
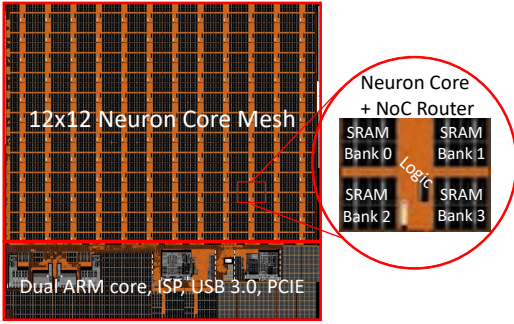
Figure 1. Taped-out 144-neuron-core SoC with SIMD execution.

This work overcomes this severe limitation. It contributes a technique that systematically exploits the translation invariance of CNN operations to make the synaptic-memory requirements independent of the neuron count. This results in extreme compression. Our technique employs two lightweight hardware blocks, a programmable event generator (PEG) and an event-to-synapse unit (ESU). The PEG computes the synaptic connectivity of thousands of neurons—grouped in a *neuron population*—using a single instruction word, the *axon*. The ESU fills the synaptic connections with weights. Weights can be shared among all neurons of a population, reducing the memory requirements for parameters.

Our proposed technique was taped-out through the 144-neuron-core *GrAI-VIP* shown in Fig. 1. In the 12-nm SoC of size $60\,mm^2$, our technique exhibits negligible implementation cost, while providing overall memory compression rates of over $300\times$ for modern CNNs compared to the best-published reference technique.

Intel recently revealed its new self-contained and event-based deep-neural-network (DNN) accelerator *Loihi 2*. It is capable to run *Nvidia*'s *PilotNet* CNN in $30\,mm^2$ using its 7-nm technology [2]. The same network (i.e., without any extra optimizations) requires only 3 out of 144 cores on our chip using a larger technology node at $2\times$ the die area. This demonstrates the practical value of the proposed technique, as it allows event-based cores to run much more sophisticated/complex CNNs in a temporal-sparse fashion on a single low-cost, self-contained, and event-based accelerator.

The rest of this paper is structured as follows. Related work is discussed in Section 2. Section 3 includes the preliminaries covering CNNs and their sparse execution on event-based accelerators. The proposed technique is derived in Section 4. Section 5 includes discussions and experimental results. Finally, a conclusion is drawn.

2 RELATED WORK

This section reviews related work on event-based architectures and memory-footprint compression. A wide range of massively parallel, self-contained, event-based architectures have been proposed (e.g., [2]–[4], [6]–[8], [11]). Most only support neuromorphic neuron models, while *GrAI Matter Lab*'s *Neuronflow* architecture [3] and the *Loihi2* [2] support also traditional DNNs—executed in a time-sparse manner to reduce the compute requirements [3], [5]. Such DNNs are today more accurate and easier to train.

Reducing the memory footprint of neural networks is an actively researched topic. Compression is vital for self-contained architectures, as non-fitting CNNs cannot be supported. Traditional architectures have looser memory constraints due to the usage of external DRAM. However, even here compression has great advantages, as it reduces latency- and power-hungry DRAM accesses [12].

One approach to reducing memory requirements at the application level is to use a lighter-weight CNN (e.g., [9], [13]). Another possibility is to execute a given CNN at a lower precision. A common technique is to run the network in 8-bit integer arithmetic [14], but even binary network implementations exist [15]. *Han et al.* proposed to iteratively prune weights with a small magnitude (effectively setting them to 0), followed by incremental training to recover accuracy [12]. In combination with 8-bit integer arithmetic and weight entropy-encoding, weight pruning can achieve compression rates larger than $10\times$ for modern CNNs [12].

The approaches mentioned above do not only reduce the memory footprint, but also the computational complexity of the CNN inference. Also, since these techniques transform the neural network itself, they are effective for most compute architectures. The drawback is that the techniques are *lossy*; i.e., they typically entail some accuracy loss that is partially recoverable by retraining [12], [14].

Synapse-compression techniques for event-based systems, such as the one proposed in this work, are *orthogonal* to the *lossy* techniques discussed above. Hence, both compression types can be applied in conjunction and studied independently. Since synapse-compression techniques are *lossless*, they do not affect the network prediction/output. Hence, these techniques, tailored for event-based systems, entail no loss in network accuracy. Thus, they can be applied post-training.

Early event-based architectures used a single routing LUT in the source to look up all synaptic connections of a neuron on its firing [6]. This approach results in many events and large memory requirements for DNNs with many neurons, $|\mathcal{N}|$, as the number of required bits is of complexity $\mathcal{O}(|\mathcal{N}|\log_2(|\mathcal{N}|))$. *Moradi et al.* and *Davies et al.*, independently, found that the events can be reduced and the synaptic-memory compressed to $\mathcal{O}(|\mathcal{N}|\sqrt{\log_2(|\mathcal{N}|)})$ through a hierarchical, tag-based routing scheme [6], [8]. This hierarchical routing scheme found application in *Intel*'s original *Loihi* architecture and the *DYNAPs* architecture.

The technical note of the recently released *Loihi 2* claims that the synaptic memory footprint for CNNs has been compressed again by up to $17\times$ [2]. Unfortunately, details of the approach are (at the time of writing) not fully disclosed. However, at a reduction of up to $17\times$, the synaptic memory requirements must still be at least of complexity $\mathcal{O}(|\mathcal{N}|)$. Thus, larger CNNs would remain unfeasible for *Loihi2*.

The idea of generating a synaptic memory structure for event-based CNN inference that scales independently of $|\mathcal{N}|$ (required to run today's complex CNNs), has been tried for the *SpiNNakker* chip [16]. However, the existing method is not generic enough. It only supports simple convolution layers. Other common CNN operations such as stride-2 convolutions, polling, and depth-wise convolutions are all not supported. Moreover, the technique does not allow the cutting of feature maps (FMs) in multiple fragments for

compute or memory load-balancing. Hence, the technique was only demonstrated in Ref. [16] to work for a tiny CNN with five standard convolution layers and a maximum feature shape of 28×28. Thus, it cannot be implemented for modern deep CNNs which include many more layer types. Moreover, modern CNNs have large FM dimensions and strongly heterogeneous compute requirements per layer which make FM-cuts inevitable. Thus, the problem addressed by this work remained unsolved until this point.

3 PRELIMINARIES

3.1 Neural Networks

In neural networks for image processing, a *neuron population* is represented by a three-dimensional matrix, $\mathbf{P} \in \mathbb{R}^{D \times W \times H}$. The last two dimensions determine the 2D Cartesian-grid position to correlate a neuron with a location in space; the first coordinate indicates the feature (or channel) that is sampled. Thus, a single neuron population represents multiple features. Here, the number of channels of such a multi-channel FM is denoted as D. The 2D submap of channel c_i ($\mathbf{P}_{c,x,y}|_{c=c_i}$) has the dimensions of a single feature, defined by a tuple: width, W, and height, H.

The raw input image represents the input population of the network. For example, a 300×300 *RGB* image is represented by a $3 \times 300 \times 300$ $\mathbf{P}$ matrix, where $\mathbf{P}_{c,x,y}$ is the pixel value for color channel c at location (x, y). Starting with this input population, new FMs are extracted out of the existing FMs successively (feed-forward structure). One such extraction step is symbolized as a network layer in a dataflow graph structure. The most intuitive form is a fully connected layer, in which each neuron in the destination FM, $\mathbf{P}^+$, is a function of all neurons in a source FM, $\mathbf{P}$:

$$\mathbf{P}^+_{c,x,y} = \sigma \left(\sum_{i=0}^{D-1} \sum_{j=0}^{W-1} \sum_{k=0}^{H-1} \mathbf{W}_{c,x,y,i,j,k} \mathbf{P}_{i,j,k} + b_c \right). \quad (1)$$

Here, b_c is the bias of the neurons of feature c, and $\mathbf{W}$ is the weight matrix. A DNN can be implemented in its traditional form or as a spiking leak-integrate-fire neural network (LIF-NN). In the first variant, $\sigma()$ is a non-linear activation function to enable non-linear feature extraction. Often, a rectifier/*ReLU* is used, clipping all negative values to zero. The *ReLU* function exhibits low hardware complexity. Neuromorphic LIF-NNs differ from traditional DNNs through a more complex, stateful activation, $\sigma()$, with periodic state-leakage.

A major problem with fully connected layers is the large number of synaptic weights which determine the compute and memory requirements. For example, extracting ten 300×300 features from a $3 \times 300 \times 300$ FM requires 243 M weights and multiply-accumulate (MAC) operations.

This can be overcome by exploiting *spatial locality* [17]. For a meaningful feature extraction, it is not needed to look far in XY to glean relevant information for one XY coordinate of the extracted feature. Thus, outside a relative range of XY size (KW, KH)—denoted as the receptive field—all synapses between neurons are removed. This drastically reduces the compute and memory requirements for such *locally connected* 2D layers.
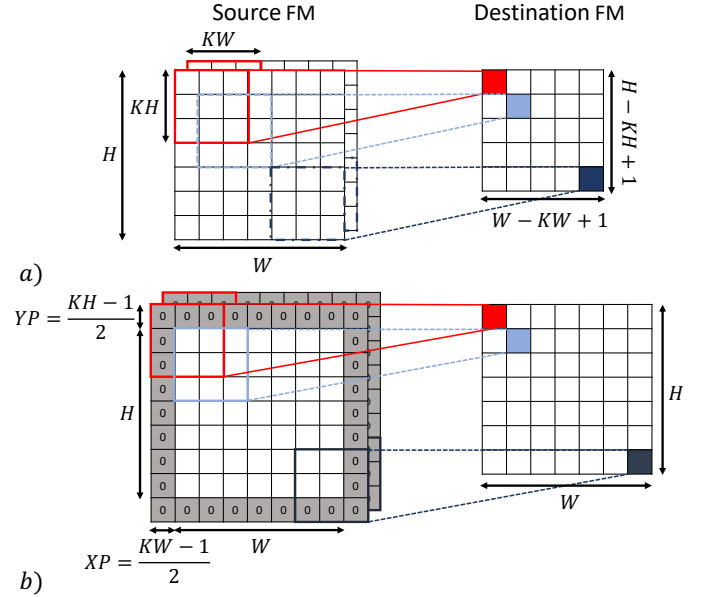

Figure 2. Convolution operation without padding (a), and with "same" zero-padding (b) resulting in no resolution reduction.

Moreover, network filters should respond similarly to the same patch, irrespective of its XY location in the source FM. This principle is called *translation invariance* [17]. Hence, the relative weights can be independent of the XY location of the destination neuron; i.e., weights can be reused for all neurons of the same output channel. This further reduces the memory requirements.

The regular convolution operation in a CNN adds both, spatial locality and translation invariance compared to fully connected layers. This results in the following formula for a convolution layer with a kernel size of $KW \times KH$:

$$\mathbf{P}^+_{c,x,y} = \sigma \left(\sum_{i=0}^{D-1} \sum_{j=0}^{KW-1} \sum_{k=0}^{KH-1} \mathbf{W}_{c,i,j,k} \mathbf{P}_{i,x+j,y+k} + b_c \right). \quad (2)$$

The XY size of the extracted FM in a convolution operation is the XY size of the source FM minus $KW-1$ in width and $KH-1$ in height. This is the number of times the convolution kernel fits in the source FM, illustrated in Fig. 2.a. Padding rows and columns of zeros around the source is done to control the size of the output FM. To achieve an output of the same size as the input (i.e., to preserve the feature resolution), one must pad $(KH-1)/2$ rows of zeros at the top and bottom of the source FM, and $(KW-1)/2$ columns at the left and right. Fig. 2.b illustrates this zero-padding.

Instead of explicitly padding the source FM in a pre-processing step, the effect of zero padding can be expressed implicitly, by changing the source-FM indices in Eq. (2):

$$P^+_{c,x,y} = \sigma \left(\sum_{i=0}^{D-1} \sum_{j=0}^{KW-1} \sum_{k=0}^{KH-1} \mathbf{W}_{c,i,j,k} \mathbf{P}_{i,x+j-XP,y+k-YP} \right.$$
$$\left. + b_c \right) \quad \text{with } \mathbf{P}_{i,x,y} = 0 \text{ for } x < 0 \text{ or } y < 0. \quad (3)$$

Here, XP and YP are the rows/columns of zeros padded at the left and the top of the source FM, respectively.

Kernel striding and source upsampling are other ways of controlling the dimensions of the extracted features. With a stride of two, the kernel is not shifted by one step for every generated output point but by two, resulting in extracted features with a 50 % smaller resolution. When the source is upsampled to increase the resolution of the extracted features, zeros are filled between the upsampled source values followed by a trainable convolution on the upsampled map.

3.2 Event-Based Architectures

In this section, we outline the conceptual idea of event-based compute architectures for efficient CNN inference. These architectures exhibit massive parallelism with many identical cores connected through a network-on-chip (NoC) [2], [6].

To each of the C cores, one or more neuron populations, $\mathbf{P}_i$, are statically mapped. Near-memory computing is applied in the architectures. Thus, the entire memory is distributed equally over the cores, and the neural parameters (e.g., weighted synapses) are stored in the cores to which the respective neurons are mapped. The dynamic variables, computed by one core (i.e, the activated neuron states; see Eq. (3)), and needed as inputs by other cores for the calculation of neuron states, are exchanged through events over the NoC. Hence, there are no coherence problems. This allows the removal of higher/shared memory levels, improving latency and power consumption.

A drawback is that local on-chip memories have limited capacity. Thus, the static/compile-time mapping of neuron populations to cores must satisfy hard memory constraints; i.e., the number of neurons and synapses that can fit in a core is limited by the core's memory capacity. If a neuron population $\mathbf{P}_i$ of the CNN has too many parameters or neurons, it needs to be split/cut into multiple smaller populations before core assignment.

The arrival of data in form of an event triggers the compute (dataflow execution). A buffer stores the received events for FIFO processing. Event processing multiplies the event value with the weights of the synapses between the source neuron and the destination neurons mapped to the core. The results are accumulated in the destination neuron states. After accumulation, activated neuron states are sent through events to all synaptically connected neurons in the following layers. Since these neurons can be mapped to any core in the cluster, events can also be injected into the local event queue instead of going out on the NoC.

Note that above we describe how more recent architectures (considered in this paper) work. In some earlier architectures, the multiplications of activations by synaptic weights are executed at the source (i.e., before event transmission). Here, event processing at the destination only requires the addition of the event value to the target neuron state [6]. This scheme results in more events for neurons with multiple synapses. Thus, it is no longer applied in modern architectures.

3.2.1 Sparsity Exploitation in Event-Based Architectures

During DNN execution, no events are generated for zero-valued activations. Skipping zero-valued events induces no neuron-state accumulation error. Thus, each zero in an FM reduces the compute and communication requirements—saving energy and compute resources [18]. This is an advantage of event-based architectures compared to more traditional architectures. Particularly for modern CNNs with large degrees of activation sparsity (i.e., zero-valued activations), it gives event-based architectures a power-performance advantage. Standard CNNs using *ReLU* activations exhibit an activation sparsity of over 50 %, as a *ReLU* clips all negative values to zero [19]. Thus, event-based processing improves the power-delay product by about $4\times$ at no accuracy loss.

Event-based architectures exhibit even larger gains by implementing CNNs as LIF-NNs or sigma-delta neural networks (SD-NNs) to increase sparsity. A LIF-based CNN has the same synaptic connectivity as a standard CNN implementation [20]. However, LIF-NNs exhibit a more complicated firing behavior—expressed by $\sigma()$ in Eq. (3). This increases sparsity but also makes back-propagation training hard. Consequently, LIF-NNs cannot yet compete accuracy-wise with standard CNNs for complex applications.

To address this, SD-NN implementations increase the neural sparsity by transforming temporal correlation of neuron potentials between subsequent inferences into event sparsity [5]. This is particularly efficient for time-continuous input data such as video streams. By keeping memory for a persistent accumulator state for each neuron, the temporal deltas in the activations can be exchanged/processed instead of absolute values. Still, the same inference results as a standard CNN implementation are obtained as state accumulation is a linear operation. Hence, SD-NNs exhibit no training or accuracy issues. Any standard CNN can be executed as an SD-NN at no accuracy loss and without retraining. Still, SD-NNs improve sparsity noticeably. The temporal deltas of the activations exhibit more zeros than the absolute activation maps, due to the present temporal correlation—especially if activations are quantized [5]. Thereby, SD-NNs increase the gains of event-based processing without sacrificing any network accuracy.

The proposed, as well as the reference techniques, work for all three described CNN variants (standard, LIF, and SD). Thus, in the remainder of this paper, we uses the term *firing neuron* to describe a neuron of any type for which the synaptic connectivity has to be triggered due to a non-zero activation, activation-delta, or spike.

3.2.2 Synaptic-Memory in Existing Architectures

Event-based accelerators need information on the synaptic connectivity of a firing neuron to identify which neurons to update with which weights. Mathematically, the connectivity of neurons can be described as a directed graph $\mathcal{G} = (\mathcal{N}, \mathcal{S})$, where $\mathcal{N}$ and $\mathcal{S}$ are the sets of neurons and synapses, respectively. Each synapse, $s_i \in \mathcal{S}$, can be described by a tuple $(n_{\mathrm{src}}, n_{\mathrm{dst}}, w)$, where $(n_{\mathrm{src}}, n_{\mathrm{dst}}) \in \mathcal{N}^2$ is the synapse's source and destination neuron, respectively, and w is the synaptic weight.

In early event-based accelerators, LUTs store the synapse information, mapped to the cores together with the neurons. On the firing of a neuron, the addresses of the destination neurons together with the weights/parameters are looked-up, and for each pair an event carrying the firing value

multiplied by the weight is emitted towards the destination neuron. If F is the average number of outgoing synapses per neuron, the required memory bits to store the connectivity (i.e., synapses without the weights) for $|\mathcal{N}|$ neurons in this scheme is

$$Mem_{\mathrm{c}} = |\mathcal{N}| F \log_2(|\mathcal{N}|). \tag{4}$$

With B-bit weights, the parameter requirements become

$$Mem_{\mathrm{p}} = |\mathcal{N}| F B. \tag{5}$$

For modern neural networks with many neurons, a LUT results in high memory requirements. As an illustrative example, let us investigate the last 3×3 convolution of the *ResNet50* CNN [1], with $512 \times 7 \times 7$ neurons in the source and destination. Stroing the connectivity of all neurons in this layer in a LUT requires at least 110 MB. The weights would need an additional 201 MB at an 8-bit precision.

Moreover, the standard LUT-based approach has the disadvantage that it results in one event per synapse—so F events per firing neuron. A hierarchical/two-stage LUT layout reduces the number of events and the memory requirements [6], [8]. For each spiking neuron, only the addresses of the destination cores are looked up in the first routing table at the source. Thus, only one event is generated per destination core instead of one per destination neuron (while hundreds of neurons are mapped to a single core). An event contains a K-bit tag, stored also in the LUT at the source, and the firing value. In the destination core, the weights and the target neurons are selected based on the tag through a second LUT.

For a maximum of F_{max} in-going synapses per neuron, the tag-width must be at least $\log_2(F_{\mathrm{max}})$. With C cores, M neurons per core, and an average of F in-going synapses per neuron, the number of bits to store the connectivity of $|\mathcal{N}|$ neurons reduces to

$$Mem_{\mathrm{c}} = Mem_{\mathrm{c,src}} + Mem_{\mathrm{c,dst}} \tag{6}$$
$$= |\mathcal{N}| \Big({}^{F}\!/\!_{M} \log_2(F_{\mathrm{max}} C) + \log_2(F_{\mathrm{max}}) F \Big),$$

in the best case. However, the memory requirement still scales with $|\mathcal{N}|$. Thus, the scheme is still impractical for modern CNNs. Analyzing again the last 3×3 convolution layer of *ResNet50*, the synaptic memory requirement is still at least 167 MB.

4 TECHNIQUE

In the following, we propose a technique to compress the synapses for CNNs such that the memory requirements no longer scale with the neuron count but just with the population count. Fig. 3 illustrates the idea compared to the existing hierarchical-LUT scheme. We propose to use two hardware blocks, a programmable event generator (PEG) and an event-to-synapse unit (ESU) rather than LUTs.

To avoid memory requirements per neuron, so-called *axons* in the source connect entire neuron populations instead of individual neurons. For each population, $\mathbf{P}_{\mathrm{dst},i}$, with at least one synapse directing from the current population, $\mathbf{P}_{\mathrm{src},i}$, an axon is stored at the source. Axons are the PEG's "instructions", defining simple routines executed on the firing of any neuron to generate the required events. Besides
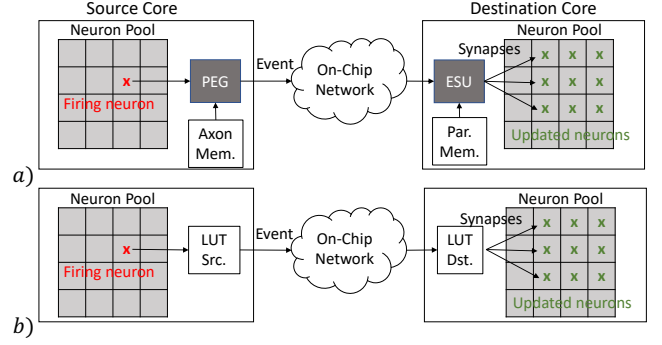

Figure 3. *a)* Proposed technique based on two hardware blocks. *b)* Reference technique based on a hierarchical LUT.
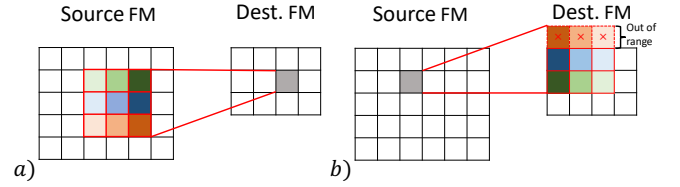

Figure 4. Regular (*a*) and event-based (*b*) convolution implementation.

the *axon(s)* of the population, the PEG needs information on the firing neuron. Like the reference technique [6], our technique results in low NoC bandwidth requirements, as the PEG generates at most one event per axon.

The ESU in the destination core decodes the event into weighted synapses. The ESU uses weight sharing between different synapses. This means that events that originate from the same FM, but from different neurons, can use the same weights without having to store them multiple times. This yields a weight compression on top of the savings provided by the axon scheme due to the translation invariance of CNN operations.

In the remainder of this section, we successively derive the architecture of the ESU and PEG to support state-of-the-art CNNs at a maximized compression rate. We start by looking at the simple case of a regular convolution. First, we assume that the compute and memory capacity of each core is large enough that it is not needed to split any multi-channel FM into several populations mapped onto different cores. Afterwards, the approach is extended to cover FM fragmentation, kernel striding, and source upsampling.

4.1 Basic Technique

To identify which outgoing synapses a firing neuron has, we must view the convolution operation in a transposed, i.e. event-based, fashion. The traditional view (illustrated in Fig. 4.a for a single channel) reduces source values via the kernel; the event-based view broadcasts source elements via the transposed kernel (illustrated in Fig. 4.b). Event processing adds the event value multiplied by the respective weight to any neuron state in the range of the transposed kernel. The final neuron states for the inference are obtained after all events have been processed.

To obtain the same final neuron states in the event-based implementation as in the standard implementation,

---

Algorithm 1 PEG for a regular convolution.

Require: Firing neuron & value: $x_{src}, y_{src}, c_{src}, v$
Require: Axon set of population: $\mathcal{A}$
 1: **for** $A = (X_{off}, Y_{off}, AD_c, ID_p) \in \mathcal{A}$ **do**
 2:    $x_{min}, y_{min} = (x_{src}, y_{src}) + (X_{off}, Y_{off})$
 3:    $gen\_event(AD_c, ID_p, x_{min}, y_{min}, c_{src})$
 4: **end for**

Algorithm 2 ESU for a regular convolution.

Require: Event body: $x_{min}, y_{min}, c_{src}, v$
Require: Neuron population & shape: $\mathbf{P}, D, W, H$
Require: Transposed weights & kernel size: $\mathbf{W}, KW, KH$
 1: **for** $\Delta x \in [0, KW)$ **do**
 2:    $x = x_{min} + \Delta x$
 3:    **continue if** $x \notin [0, W)$ // kernel part out of range?
 4:    **for** $\Delta y \in [0, KH)$ **do**
 5:       $y = y_{min} + \Delta y$
 6:       **continue if** $y \notin [0, H)$ // kernel part out of range?
 7:       **for** $c \in [0, D)$ **do**
 8:          // update_neuron depends on neuron model
 9:          $update\_neuron(\mathbf{P}_{c,x,y}, \mathbf{W}_{c,\Delta x,\Delta y,c_{src}}, v)$
10:       **end for**
11:    **end for**
12: **end for**

---

the weight arrangement for the broadcasted kernel must be transposed in XY (e.g., top-left weight becomes bottom-right) compared to the regular view. In the regular view, the destination neuron's XY coordinate is the upper-left anchor point of the kernel in the source-FM. Thus, in the event-based variant, the XY location of the broadcasted source neuron is the bottom-right anchor point of the transposed kernel in the destination FM. Equation (3) on page 3 shows that padding shifts the XY coordinate of the bottom-right anchor-point of the transposed kernel by the padding amount, (XP, YP).

Thus, on the firing of a neuron on channel c_{src} with XY coordinate (x_{src}, y_{src}), all neurons in the destination 3D FM must be updated whose X and Y coordinate is in $(x_{src}-KW+XP, x_{src}+XP]$ and $(y_{src}-KH+YP, y_{src}+YP]$, respectively. In that range, the XY-transposed kernel weights $\mathbf{W}_{i,j,k,l}|_{l=c_{src}}$ are scaled (i.e., multiplied) by the firing value and added to the respective neuron states. For some firing neurons nearby the edges of an FM, part of the broadcasted transposed kernel does not overlap with the destination FM, as illustrated in Fig. 4.b. Such kernel parts located outside the FM boundaries do not result in neuron updates. Thus, they are skipped in the ESU.

The pseudo codes in Alg. 1 and Alg. 2 describe the required functionality of the PEG and the ESU, respectively. Hardware implementation is done most efficiently through simple state machines. The PEG of the source core (i.e., the core with the firing neuron) calculates the top-left anchor point for the transposed convolution kernel in the destination FM, (x_{min}, y_{min}). As outlined above, this requires a subtraction of $(KW-XP-1, KH-YP-1)$ from the XY coordinates of the firing neuron (x_{src}, y_{src}). Since the padding and kernel shape are constant at CNN-inference-time, this is done in the PEG at once by adding a signed offset pair to the neuron's coordinates:

$$X_{off}, Y_{off} = (-KW + XP + 1, -KH + YP + 1). \quad (7)$$

Storing compile-time calculated offset values rather than the kernel shape and the padding in an axon, saves addi-

tions/subtractions in the PEG for each firing neuron as well as bits in the axon.

The outgoing event generated by the PEG contains the computed (x_{min}, y_{min}) coordinates, which can contain negative values if the top-left anchor-point is located outside the FM range. Moreover, the firing value, v, and the channel of the firing neuron, c_{src}, are added to the event body. Finally, events need the NoC address of the core to which the target population is mapped, AD_c, as well as a destination-population identifier, ID_p. The later enables that multiple populations can be mapped onto the same core. These last two parameters are static and thus part of the axons.

Each source population has an independent axon for each directly connected destination population. On each firing, the PEG must process all these axons to generate events towards all populations.

At the far end, the ESU takes the event and selects the required compile-time-transposed 3D kernel, $\mathbf{W}_{i,j,k,l}|_{l=c_{src}}$ based on c_{src} and ID_p from the event. It applies the weights scaled by the event value on the neurons with the top-left anchor point taken from the event (x_{min}, y_{min}). It skips kernel parts that are outside the population boundaries. The iteration order is channel-first (HWC). This minimizes the amount of required *continue* statements to at most $KH \cdot KW$, reducing the complexity of a hardware implementation.

The proposed technique shares kernels and axons among all neurons of a population. Hence, besides axons, neurons, and weights, we need two more types of memory words: population descriptors and kernel descriptors. A population descriptor contains the 3D neuron population shape, the neuron type incl. the activation function, the start address of the state values, and the number of axons linked to the population. A kernel descriptor contains the kernel shape, its weight width, and a memory pointer for the weights.

4.2 Support for FM Cutting

A multi-channel FM in the original/pre-mapped CNN graph can have so many parameters or neurons that it cannot be mapped onto a single core due to memory or compute constraints. Thus, the proposed technique supports the cutting of FMs into several smaller neuron populations, mapped onto different cores.

An FM cut that divides the channels results in a reduction in the number of neurons as well as weights mapped to each core. On the other hand, a cut in the XY space of the features requires all populations to contain all weights. This is due to the translation invariance of the convolution operation. Hence, a cut reducing only the X or Y size of the individual populations increases the overall memory requirements, as shared weights are duplicated (i.e., mapped onto multiple cores). Nevertheless, our approach supports both: cuts in channel coordinate C and XY. The rationale is that, for high-resolution features, it may happen that even a single channel does not fit into a core, making XY cuts inevitable. Also, addressing limitations can result in inevitable XY cuts. For example, for 8-bit population-width/height fields, a high-resolution FM has to be split into populations with a width and height of at most 255.[1]

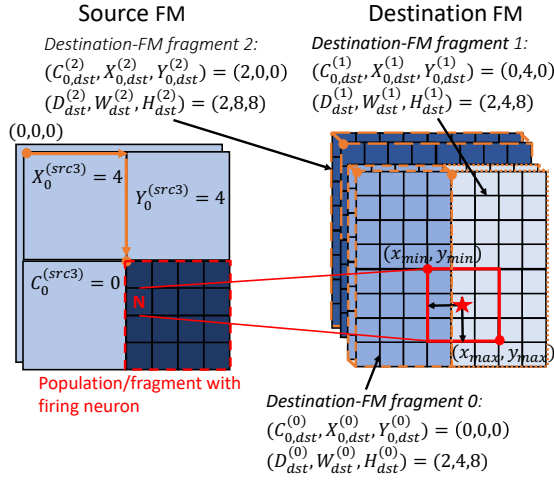1. Such fragments can be mapped to the same core to share weights.

Figure 5. Cutting of the source and the destination FM.

Fig. 5 shows an example where the source and destination FM are cut into four and three pieces, respectively. The example helps to understand the following mathematical derivation of the FM-fragmentation technique.

Let the shape of the original, unfragmented i^{th} FM be (D_i, W_i, H_i). The FM is cut into M disjoint populations $\mathbf{P}_i^{(0)}, \mathbf{P}_i^{(1)}, \ldots, \mathbf{P}_i^{(M-1)}$. The shape of the jth fragment is $(D_i^{(j)}, W_i^{(j)}, H_i^{(j)})$ and it contains all neurons from the original FM with $c \in [C_{0,i}^{(j)}, C_{0,i}^{(j)}+D_i^{(j)})$, $x \in [X_{0,i}^{(j)}, X_{0,i}^{(j)}+W_i^{(j)})$, and $y \in [Y_{0,i}^{(j)}, Y_{0,i}^{(j)}+H_i^{(j)})$. Thus, $(C_{0,i}, X_{0,i}, Y_{0,i})$ is the coordinate of the upper-left first neuron of the fragment. For a valid fragmentation, each neuron must be mapped to exactly one population. This is satisfied if the neuron-population fragments are disjoint and if the number of neurons in the pre-mapped FM is the same as the sum of the number of neurons of all generated fragments.

Next, we discuss how to adapt the PEG to cope with FM cuts. When a neuron fires in a population, its coordinates, $(c_{\text{src}}, x_{\text{src}}, y_{\text{src}})$, are the ones relative to the upper-left cut point in the original FM, not the entire FM. Thus, adding to the neuron coordinates this start point of the fragment in the original FM, $(C_{0,\text{src}}, X_{0,\text{src}}, Y_{0,\text{src}})$, results in the neuron coordinates in the original/uncut FM. Hence, the upper-left anchor point of the broadcasted kernel in the original destination FM and the channel of the firing neuron are

$$c_{\text{src,orig}} = c_{\text{src}} + C_{0,\text{src}}$$
$$x_{\text{min,orig}} = x_{\text{src}} + X_{0,\text{src}} - KW + XP + 1$$
$$y_{\text{min,orig}} = y_{\text{src}} + Y_{0,\text{src}} - KH + YP + 1. \quad (8)$$

For each fragment of the destination FM, we then calculate the location of this upper-left anchor point of the transposed kernel relative to their XY start-point in the original FM:

$$\begin{aligned}
x_{\text{min}} &= x_{\text{min,orig}} - X_{0,\text{dst}} \\
&= x_{\text{src}} + X_{0,\text{src}} - KW + XP + 1 - X_{0,\text{dst}} \\
y_{\text{min}} &= y_{\text{min,orig}} - Y_{0,\text{dst}} \\
&= y_{\text{src}} + Y_{0,\text{src}} - KH + YP + 1 - Y_{0,\text{dst}}. \quad (9)
\end{aligned}$$

These $(x_{\text{min}}, y_{\text{min}})$ coordinates, together with $c_{\text{src,orig}}$, are sent via an event to the core of the destination-FM fragment.

All parameters but the coordinates of the firing neuron in Eq. (9) are constants at run-time. Thus, supporting FM cuts just needs an adjustment of the X and Y offset values calculated at compile time, plus an additional offset value for the channel coordinate:

$$\begin{aligned}
C_{\text{off}} &= C_{0,\text{src}} \\
X_{\text{off}} &= X_{0,\text{src}} - KW + XP + 1 - X_{0,\text{dst}} \\
Y_{\text{off}} &= Y_{0,\text{src}} - KH + YP + 1 - Y_{0,\text{dst}}. \quad (10)
\end{aligned}$$

Note that the offset values for X and Y can be negative here. Thus, they are signed values. The channel offset is always positive. Hence, it can be an unsigned value.

For each population/FM-fragment pair that is connected by at least one synapse, an axon is needed. However, the number of axons remains minimal, as different populations are mapped onto different cores. Thus, different axons are required anyway due to the different core addresses.

Each core only stores the weights for the channels that are mapped to it. Thus, the indices of the weight matrix are relative to the first channel of the respective fragment; i.e., when neurons of the channels 4 to 7 are mapped onto a core, $\mathbf{W}_{0,0,0,0}$ stored in the local core memory is the upper-left kernel weight for source channel 0 and destination channel 4 of the original transposed weight matrix. This fragmentation of the weight matrix is done entirely at compile time.[2]

In summary, besides an additional axon parameter C_{off} added to the channel coordinate, nothing is added to the PEG hardware. The ESU must not be modified at all.

There is an optional extension to the PEG. A *hit detection* to filter out events that an ESU decodes in zero synapses as the kernel does not overlap at all with the destination population. Consider in Fig. 5, that the neuron at position (0,1,1) instead of (0,0,1) fires. The PEG depicted by Alg. 1 sends an event to the core, destination-FM fragment 0 is mapped onto. This event has an x_{min} value of 4. However, the population only contains neurons with $x \in [0, 3]$. Thus, event decoding by the ESU at the receiving side results in no activated synapse (i.e., *continue* in line 3 of Alg. 2 always triggered). The system functions correctly without an extension. However, transmitted events yielding no activated synapses after decoding increase the energy and processing requirements unnecessarily. Such events are best filtered out by the PEG in the source already.

This PEG power-performance optimization is achieved by calculating not only the XY start-coordinate of the projected kernel (i.e., the top-left anchor point) but also the first X and Y coordinates outside the range. These coordinates are $(x_{\text{min}}, y_{\text{min}}) + (KW, KH)$. One can then check if the kernel overlaps with at least one neuron of the population through simple Boolean operations. If it does not, no event is generated. To enable this optimization, axons must contain the kernel shape as well as the width and height of the destination population.

Hit detection in the channel coordinate is not required, as all channels in the XY kernel range are updated at the destination, irrespective of the channel of the firing neuron. Thus, if cutting in XY is the rare exception, hit-detection support might be skipped to reduce cost. However, hit detection has a reasonable hardware cost. Hence, hit-detection

2. All weight sets are only disjoint for no X or Y cuts.

Algorithm 3 PEG for a regular convolution with support for FM fragmentation and empty-event skipping.

Require: Firing neuron & value: $x_{\text{src}}, y_{\text{src}}, c_{\text{src}}, v$
Require: Axon set of population: $\mathcal{A}$
1: // grayed hit-detection only needed with many XY cuts
2: **for** $(X_{\text{off}}, Y_{\text{off}}, C_{\text{off}}, W, H, KW, KH, AD_{\text{c}}, ID_{\text{p}}) \in \mathcal{A}$ **do**
3: $\quad x_{\min}, y_{\min}, c_{\text{src}} = (x_{\text{src}}, y_{\text{src}}, c_{\text{src}}) + (X_{\text{off}}, Y_{\text{off}}, C_{\text{off}})$
4: $\quad x_{\max}, y_{\max} = (x_{\min}, y_{\min}) + (KW, KH)$
5: $\quad$ **if** $(x_{\min} < W) \,\&\, (x_{\max} > 0) \,\&\, (y_{\min} < H) \,\&\, (y_{\max} > 0)$ **then**
6: $\quad\quad gen\_event(AD_{\text{c}}, ID_{\text{p}}, x_{\min}, y_{\min}, c_{\text{src}})$
7: $\quad$ **end if**
8: **end for**

Algorithm 4 ESU with support for strided convolutions.

Require: Event body: $x_{\min}, y_{\min}, c_{\text{src}}, v$
Require: Neuron population & descriptor: $\mathbf{P}, D, W, H$
Require: Trans. weights & descriptor: $\mathbf{W}, KW, KH, SL$
1: **for** $\Delta x \in [0, KW)$ **do**
2: $\quad x = x_{\min} + \Delta x$
3: $\quad$ **continue if** $x \notin [0, W)$ **or** $x \,(\text{mod } 2^{SL}) \neq 0$
4: $\quad$ **for** $\Delta y \in [0, KH)$ **do**
5: $\quad\quad y = y_{\min} + \Delta y$
6: $\quad\quad$ **continue if** $y \notin [0, H)$ **or** $y \,(\text{mod } 2^{SL}) \neq 0$
7: $\quad\quad x, y = (x, y) \gg SL$ // XY down-sampling
8: $\quad\quad$ **for** $c \in [0, D)$ **do**
9: $\quad\quad\quad update\_neuron(\mathbf{P}_{c,x,y}, \mathbf{W}_{c,\Delta x, \Delta y, c_{\text{src}}}, v)$
10: $\quad\quad$ **end for**
11: $\quad$ **end for**
12: **end for**

---

support is beneficial in most cases. Alg. 3 shows the pseudo code for the PEG with support for FM fragmentation and hit detection.

4.3 Down- and Upsampling Support

In the following, we extend the PEG-ESU pair to support upsampling and strided convolutions. A kernel stride of N in a convolution implies that the anchor point of the kernel in the regular/output-centric view (cf. Fig. 4.a) is advanced by N in X between two generated output points. Once the end of a line is reached, the anchor point is advanced by N in Y while X is reset to 0. Consequently, a kernel stride of N in a convolution results in the same extracted FM as applying the convolution kernel regularly (i.e., with a stride of 1), followed by downsampling the resulting FM by a factor N in X and Y.[3] This "destination-downsampling view" of a convolution stride is used to derive our technique.

The pseudo-code of the ESU with support for programmable kernel striding is shown in Alg. 4. We add a field SL, containing the $\log_2$ of the applied kernel stride, to the kernel descriptor. Through SL, the ESU knows which rows and columns to skip as they are gone after down-sampling such that there is no need to update a neuron state. Thus, our stride implementation based on destination downsampling results in no compute overhead as accumulation for neurons removed by downsampling is skipped.

The PEG still behaves as it would for stride-1 convolutions. Hence, the widths W and heights H of the destination fragments in the axons are the ones that would be obtained for a stride of 1. Thus, the physical width and height of the true/final downsampled FM shifted left by SL ($W_t \ll SL$

---
3. Downsampling by a factor N means here simply keeping only every N^{th} row and column.

---

and $H_t \ll SL$) are stored in the axon as W and H. This inverses the downsampling effects. Also, the offset values are adjusted to account for the destination-FM downsampling:

$$X_{\text{off}} = X_{0,\text{src}} - KW + XP + 1 - (X_{0,\text{dst}} \ll SL)$$
$$Y_{\text{off}} = Y_{0,\text{src}} - KH + YP + 1 - (Y_{0,\text{dst}} \ll SL). \quad (11)$$

All this only affects constant parameters stored in the axons. Thus, the PEG hardware remains unchanged.

Also, the ESU initially behaves as for a regular convolution. Thus, also here the true population width and height shifted left by SL are stored in the descriptor as W and H, respectively. The effective downsampling after convolution due to the kernel stride is considered by extending the *continue* conditions. In detail, if the *for-loop* iteration over the transposed kernel is at a row or column removed by the downsampling, synapse generation is skipped. Rows and columns that are not skipped are only the ones with X or Y coordinates which are 0 modulo 2^{SL}. For non-skipped kernel parts, the downsampling of the XY coordinate is applied for the selection of the neuron to be updated. This down-sampling is realized in hardware at a low cost through a right shift by SL.

Adding stride support does not add noticeably to the complexity of the ESU. First, checking that a binary signal is not 0 in modulo 2^{SL} just requires a logical *OR* operation of the last SL bits. Moreover, all common CNNs only use strides of 1 or 2. Thus, we propose to keep SL a 1-bit value such that a stride of 1 (regular convolution) or 2 can be applied in a single step. Larger strides can still be implemented by inserting dummy/identity layers with another stride of two until the needed downsampling rate is reached. This follows the architectural principle of optimizing for the common case, with non-optimized support for the uncommon case. With a 1-bit SL field, checking that a signal is not 0 modulo 2^{SL}, requires only a single *AND*-gate with the SL bit and the signal's LSB as the two binary inputs. Moreover, with a 1-bit SL value, a shift left by SL has a negligible implementation cost. It can be synthesized in a single 2-to-1 multiplexer with SL as the select signal. Thus, the hardware cost for adding stride support is low.

Next, we discuss the PEG changes to support upsampling the source before a convolution operation is applied. This is required for example for fractionally-strided convolutions [21]. Upsampling requires filling zeros between the upsampled source values. Source upsampling is realized in the PEG by shifting the XY coordinates of the firing neuron left by the $\log_2$ of the upsampling factor US before adding the offset values. Also, the X and Y offsets calculated at compile-time must consider the upsampling of the source:

$$X_{\text{off}} = (X_{0,\text{src}} \ll US) - KW + XP + 1 - (X_{0,\text{dst}} \ll SL)$$
$$Y_{\text{off}} = (Y_{0,\text{src}} \ll US) - KH + YP + 1 - (Y_{0,\text{dst}} \ll SL). \quad (12)$$

The resulting final pseudo code of the PEG with upsampling support is shown in Alg. 5.

5 DISCUSSIONS & EXPERIMENTAL RESULTS

In this section, the proposed technique is evaluated through experimental results. Furthermore, we discuss the universal

Algorithm 5 PEG with upsampling support.

Require: Firing neuron & value: $x_{\text{src}}, y_{\text{src}}, c_{\text{src}}, v$
Require: Axon set of population: $\mathcal{A}$
1: // grayed hit-detection only needed with many XY cuts
2: **for** $(X_{\text{off}}, Y_{\text{off}}, C_{\text{off}}, W, H, KW, KH, US, AD_{\text{c}}, ID_{\text{p}}) \in \mathcal{A}$ **do**
3:      $x_{\text{src}}, y_{\text{src}} = (x_{\text{src}}, y_{\text{src}}) \ll US$ // XY up-sampling
4:      $x_{\min}, y_{\min}, c_{\text{src}} = (x_{\text{src}}, y_{\text{src}}, c_{\text{src}}) + (X_{\text{off}}, Y_{\text{off}}, C_{\text{off}})$
5:      $x_{\max}, y_{\max} = (x_{\min}, y_{\min}) + (KW + KH)$
6:      **if** $(x_{\min} < W)\,\&\,(x_{\max} > 0)\,\&\,(y_{\min} < H)\,\&\,(y_{\max} > 0)$ **then**
7:          $gen\_event(AD_{\text{c}}, ID_{\text{p}}, x_{\min}, y_{\min}, c_{\text{src}})$
8:      **end if**
9: **end for**

---

usability of the technique.

As stated before, the proposed synapse compression technique is *lossless*. Hence, it has no impact on the accuracy or prediction quality of the CNNs to be executed. Thus, this section does not discuss network accuracies as the accuracies reported in the original papers of the investigated CNNs can be matched.

The derivation of our proposed technique only considered some of the layer types/operations found in modern CNNs. Thus, this section first discusses how the technique is used to implement the various additional layer types. Afterwards, we discuss silicon-implementation results. Finally, we determine the compression gains for state-of-the-art CNNs through experimental results.

5.1 Implementing Various Layer-Types

Today's CNNs contain various layer types beyond the ones that were considered for the derivation of the proposed technique in Section 4. Still, our technique based on a PEG-ESU pair is able to support them, as shown in the following for the most relevant examples.

Deconvolutions (Transposed Convolutions): Deconvolutions are used to inverse convolution operations. They are typically implemented as a transposed convolution operation shown in Fig. 4.b with the addition that the source padding and destination FM size is adjusted such that the transposed kernel always fully overlaps with the destination FM. Thus, transposed convolutions are naturally supported by the proposed technique.

Concatenation & Split Layers: Some neural networks have multiple branches that are at some point concatenated into one. This concatenation and splitting can be implemented through the PEG due to the support of FM fragmentation, described in Subsection 4.2.

Dilated Convolutions: Dilated convolutions are used to increase the receptive field of the kernel without increasing the number of trainable parameters. The idea is to add holes/zeros between the trainable weights of the kernel. The number of skipped locations in X or Y between two trainable weights is called the *dilation rate*. Hardware support for efficient dilated convolutions can be easily added. However, dilated convolutions are not found in most modern CNNs. Hence—based on the architectural principle to only optimize for the common case—we propose to implement dilated convolutions, simply as regular convolutions. If DR is the dilation rate, the used regular convolution kernel has an XY shape of $(DR \cdot KW - DR + 1) \times (DR \cdot KH - DR + 1)$. In this kernel, zeros are inserted at the intermediate positions between the learned weights. Ideally,

this is paired with an efficient zero-weight skipping technique as it is done in our silicon implementation presented in the next subsection. Note that zero skipping furthermore enables an additional drastic weight compression through pruning. Thus, zero-skipping support is typically anyway desired [22].

Depthwise & Grouped Convolutions: A depthwise convolution is a lightweight filtering, applying a single convolution per input channel (i.e., no channel mixing; i^{th} output channel only depends on i^{th} input channel instead of all). In a grouped convolution, each output channel depends on a small set of D_{group} input channels. Depthwise and grouped convolutions can be implemented with the PEG-ESU pair by splitting the original source and destination FM into many FMs of depth 1 (depthwise) or D_{group} (grouped), with regular convolution operations between the source-destination pairs covering the same channel(s).

Average & Max. Pooling: Pooling operations are implemented as strided depthwise convolutions. For example, an average pooling over non-overlapping 2×2 windows is simply a stride-2, depthwise, 2×2 convolution. Thereby, all four weights are $1/4$. Max. pooling has the same connectivity. The only difference is that the weights are 1 rather than $1/\text{PoolingWindowSize}$. Thus, only the neuron-update routine is changed for max. pooling, not the proposed synapse compression technique.

Dense Layers: A fully-connected layer from N to N^+ neurons is the same as a 1×1 convolution between two FMs of shape $N \times 1 \times 1$ and $N^+ \times 1 \times 1$. This is naturally supported by the proposed techniques. In this case, each neuron forms an individual feature. Thus, all neurons in the destination population depend on all neurons in the source population.

Flattening & Global Pooling: Flattening an FM of shape $D \times W \times H$ followed by a dense layer with N neurons (i.e., destination FM shape is $N \times 1 \times 1$) is implemented as a single regular convolution with a kernel XY shape equal to (W, H) with N output channels. Thereby, the two layers are merged into a single operation which saves compute and events. Global pooling is realized in the same fashion, only that a depthwise connectivity must be implemented.

Nearest-Neighbor & Bilinear Interpolation: An upsampling together with an interpolation requires combining the upsampling feature with an untrainable depthwise convolution representing the interpolation between the upsampled points.

Add and Multiply Layers: Add layers and pointwise multiply layers require two individual source FMs of the same shape pointing to the same destination FM. Between the two individual source FMs and the destination FM the same pointwise synaptic connectivity is required. This is implemented as the connectivity of a depthwise 1×1 convolution with a weight of 1 shared by both source FMs.

5.2 Silicon Implementation

A variant of the PEG-ESU pair supporting all layer types is implemented in our next-generation *GrAI* architecture, taped-out in the TSMC12 FinFET technology. The heart of the $60 \, \text{mm}^2$ SoC (shown in Fig. 1 on page 2) is a self-contained, event-based accelerator, supporting standard DNNs, LIF-NNs, and SD-NNs with over 18 million neurons.

The individual cores are arranged as an XY mesh connected through an NoC. By using an 8-bit relative core address (4-bit X, 4-bit Y), a neuron can have a synaptic connection with any neuron in the same core or any of the nearest 255 cores, while enabling the architecture to theoretically scale to an arbitrary number of cores. Our pre-product chip for embedded applications has 144 cores per die, but chip tiling—enabled by the relative addressing scheme—still allows for meshes with larger core counts.

Due to the self-contained nature, all neurons, weights, and other parameters mapped to a core must fit into the on-chip SRAMs. Each core contains 256 kB of unified local memory (with 64-bit words and 15-bit addresses) that can be allocated freely to weights, neuron states, and connectivity.

To utilize the memory optimally, the architecture uses 8 bits to describe the width and height of a neuron population and 10 bits to describe the depth. This is enough for modern CNNs. Larger populations can still be realized through FM cutting. The addressing allows a single population to fit over 1 million neurons. Still a neuron-population descriptor containing width, height, depth, neuron type, activation function, axon count, and start address of the population in the memory fits in one 64-bit word. Note that in our silicon implementation axons and states are stored in a continuous block. Thus, we can store only the axon count instead of a 15-bit pointer in the population descriptor, which saves bits.

The kernel width, KW, and height, KH, in the axons and kernel descriptors are 4-bit numbers. The selection of the bit widths used for kernel width and height are important design choices. Together with the width of an XY coordinate (here 8 bit), they determine the width of most data-path components in ESU and PEG. Moreover, they determine the maximum range of the *for loops* implemented through the control path.

We found that rarely a CNN has a kernel size larger than *16*. Hence, the used 4 bits do not only yield a low hardware complexity but also an efficient support of most CNNs. Note that, due to the flexibility provided by the offset fields X_{off} and Y_{off}, any larger kernel size can still be implemented through multiple axons and weight matrices. For example, a 32×16 convolution is realized as a 16×16 convolution paired with another 16×16 convolution between the same FMs for which the X_{offset} is increased by 16. The upsample and stride fields are 3 bits and 1 bit wide, respectively—enough for all common CNNs. Nevertheless, larger up- and downsample factors can be realized by adding dummy layers with an identity weight matrix.

With 8-bit XY coordinates and 4-bit kernel dimensions, X_{off} and Y_{off} are 9-bit signed values. We constrain FM fragments created by the mapper to have a width and height of at least 8 neurons (except for the last remaining cuts towards the left and bottom). This allows reducing the bit width for W and H in the *axons* and the hardware complexity of the hit detection. In practice, this implies no limitation. The reason is that the fragmentation by channels is not limited, which is strongly preferred anyway.

Given all that, also an axon and a kernel descriptor fit comfortably into a single 64-bit word. We made the design choice to have a kernel descriptor per channel of the source FM instead of only one per FM. Thus, c_{src} of the event is used besides ID_p to select the kernel descriptor. A kernel descriptor contains the 3D kernel shape (KD, KW, KH), and a pointer to the start address of the resulting 3D sub-weight-matrix, $\mathbf{W}_{sub,c_{src}} = \mathbf{W}_{i,j,k,l}|_{l=c_{src}}$, in the memory. Moreover, the kernel descriptor contains information required for zero-weight skipping and weight quantization, which is not relevant to the synapse-compression technique.

Multiple kernel descriptors per layer enable weight reuse among different source channels as well as different quantization and pruning schemes for each sub-weight matrix. Also, it overcomes the need to calculate the start point in the weight matrix the descriptor points at. All weights in the sub-matrix are traversed on an event processing. The drawback is a slightly reduced compression as we need at least C_{src} rather than one kernel descriptor per layer.

Each neuron can have a persistent state for SD-NN or LIF-NN inference, or can dynamically allocate a temporary accumulator state for regular DNN implementations. Dynamic state allocation allows mapping CNNs with larger neuron counts, as state entries can be shared among neurons whose accumulation phases are mutually exclusive. A state is a 16-bit float number for maximum precision, while a weight can be quantized to 8 bits or even less with no noticeable performance loss using adaptive-float quantization [23].

Other than that, the architecture supports multi-threading, single-instruction-multiple-data (SIMD) execution, as well as a wide range of neuron types and activation functions. Also, ESU and PEG still support absolute/non-compressed synapses for smaller network layers with irregular connectivity.

5.2.1 Impact on Power, Performance, and Area

In the following, we summarize the results of the physical implementation in the 12-nm technology. The ESU and PEG take in total less than 2 % of the area of a processor node. Only a marginal fraction ($\ll 1\%$) of the power consumption is due to the ESU or the PEG, which are also not found to be part of the critical timing path. Note that the implemented ESU and PEG include many additional features beyond the scope of this paper. Examples are support for multi-threading, weight quantization plus zero skipping, and non-compressed synaptic connectivity. Thus, the hardware costs of the proposed technique are negligible.

In line with previous work [12]—and despite applying the synapse compression—area, power, and timing of the chip are dominated by the on-chip memories used to store the parameters, neuron states, and connectivity. The memories take over 70% of the core area as shown in Fig. 1 on page 2. Thus, the power and area savings of the proposed technique are determined by the memory savings, investigated in the next subsection.

5.3 Compression Results

Through a Python tool, the memory savings of the proposed synapse-compression technique are quantified. The tool calculates the synaptic memory requirements of a given CNN for the proposed method, a simple LUT approach, and the hierarchical-LUT approach [6], [8]. For the proposed technique—other than for the reference techniques—the memory requirements of a layer increase with the number

Table 2
Bit width of instances of the data types in the various synapse compression techniques used for the experimental results.

Technique	Neurons	Parameters	Connectivity
This work	16 b	8 b	**Axons:** 64 b **Kernel Descriptor:** 64 b **Population Descriptor:** 64 b
LUT [10]	16 b	8 b	**LUT Entry:** 23 b *(8 b Core Address + 15 b Neuron ID)*
Hier. LUT [6], [8]	16 b	8 b	**Source LUT Entry:** 23 b *(8 b Core Address + 15 b Tag)* **Destination LUT Entry:** 15 b *(Neuron ID)*

of fragments the layer is split in. Thus, the tool calculates the memory requirements for the proposed scheme considering FM cuts that ensure that the total memory footprint of each resulting fragment is below 256 kB, the single core limit of our chip. By considering the real (non-beneficial) required FM cuts for the proposed technique, we report realistic rather than optimistic gains for the proposed technique.

To enable a detailed analysis, the memory requirements are categorized into *neurons, connectivity*, and *parameters*. The reported values for *connectivity* are the bits required to store the connectivity between the neurons, but they do not include the weights of the synaptic connections. Thus, for the proposed technique, it includes axons, kernel descriptors, and population descriptors. The category *parameters* includes the weights. The last section, *neurons*, reports the memory allocated for neuron states. Throughout this section, we assume that a persistent 16-bit state is allocated for each neuron in a population. Reporting the memory usage in these categories allows to access the gains of pattern/weight sharing and axon-based synapse computation in isolation. The former technique reduces the *parameter* requirements, while the latter reduces the *connectivity* requirements.

In the experiments, the tag width in the reference hierarchical-LUT technique is 15 bits. This is the minimum tag width required by the scheme to be able to map all CNNs analyzed in this section, as the analyzed networks have neurons with a fan-in (i.e., number of incoming synapses) of up to $7^2 \cdot 512$. Thereby, we present best-case values for the hierarchical-LUT reference technique, which in this form is only able to support CNNs with synaptic fan-ins of at most 32 k.

The unified memory can theoretically fit 2^{17} 16-bit neuron states in 256 kB of unified memory. Still, for the naive LUT technique, we consider only 15-bit neuron addresses, as none of our experiments resulted in a core memory that is occupied more than 25 % by neurons for this technique. Hereby, we ensure a fair comparison also for the second reference technique. Table 2 summarises again the bit widths of all data types for the three techniques.

By considering persistent 16-bit states for each neuron but 8-bit weights/parameters, we present pessimistic compression gains for the proposed technique. Our technique heavily compresses the *parameters* and the *connectivity* compared to the reference techniques but not the *neurons*. Generally, both, the effectively required bits per neuron and per parameter can be reduced further by compression

techniques orthogonal to the one proposed in this work (e.g., non-persistent states, weight pruning, entropy coding, channel pruning) [12], [24]. However, reducing the memory footprints of neurons and parameters would automatically increase the compression gains of our proposed technique. The heavily compressed connectivity in our scheme would have a higher impact in this case.

Through this pessimistic experimental setup, we ensure that the reported gains of our technique are realistically achieved in practically all applications of event-based architectures. On the downside, the setup results in pessimistic total memory requirements, why the reported values allow no final conclusion on the mappability of the analyzed CNNs on our chip. Thus, the reported memory requirements are above what is realistically achieved in our chip, which also supports many parameter and neuron compression schemes orthogonal to the proposed technique.

5.3.1 Small CNNs

We start by analyzing a relatively small CNN for today's standards, *PilotNet* [10]. It is a 9-layer CNN used for autonomous steering. This example is discussed in-depth first, as it allows us to understand the advantages as well as challenges revealed by the proposed technique. Also, *PilotNet* is the network that was demonstrated to fit in *Intel*'s newest event-based architecture, *Loihi 2*, making it a good reference benchmark. In the following subsection, we will validate the findings for more modern (and much larger) networks.

We calculate the memory requirements of each layer for the proposed and the two reference techniques. The results are plotted in Fig. 6. They show that the memory requirements of the two other published techniques are dominated by *connectivity*. For the two reference techniques LUT and hierarchical LUT 74.1 % and 65.2 % of the memory requirements are due to *connectivity*, respectively. The *parameters* are the second dominant factor for the memory requirements of the reference techniques, contributing about 25 % to 35 % to the total memory usage. For non-quantized 16-bit weights, the *parameter* requirements would compete with the *connectivity* requirements.

Despite allocating a 16-bit state per neuron, the *neurons* only account for 0.2 % to 0.3 % of the memory requirements for the reference techniques. This proves that synapse compression—as done by the proposed technique—is the most effective way to reduce the memory requirements for event-based architectures at no accuracy loss.

The proposed synapse-computation methodology drastically reduces the *connectivity* and *parameter* requirements by a factor of 15.6 k × and 107 ×, compared to the best previously published method. *Intel* reports for the upcoming *Loihi 2* architecture a CNN synapse compression of up to 17 ×.[4] The synapses, i.e., the combination of *parameters* and *connectivity*, are compressed by the proposed technique by a factor of 305 ×. This means an additional compression by a factor of 18 × on top of the 17 × published by *Intel* [2].

Connectivity, from being the biggest contributor to the memory requirements, effectively becomes negligible with

---

4. As of writing this paper, only maximum compression results are available for *Loihi 2* [2]. The details of the used technique are not fully disclosed. Thus, more comparisons with *Loihi 2* cannot be drawn.
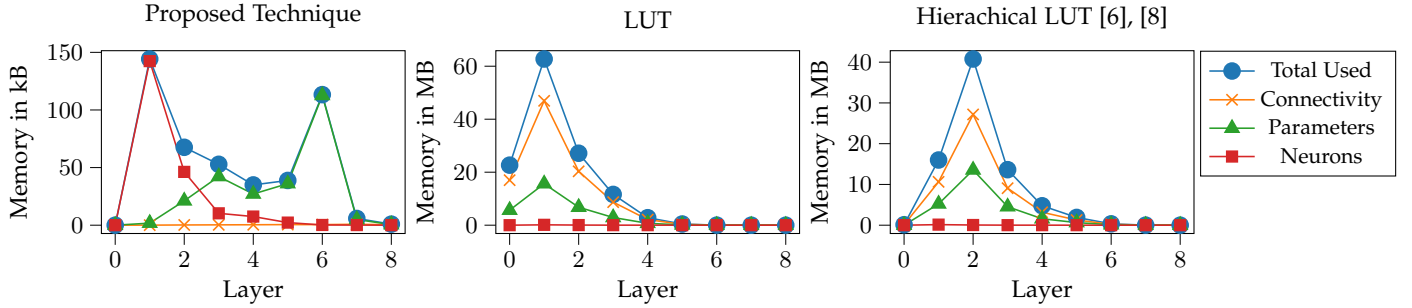
Figure 6. Memory requirements for *PilotNet* [10] with the proposed and reference techniques. Note the different Y scale (kB vs. MB).

the proposed technique, contributing only 0.7 % to the memory usage. *Parameters*, on the other hand, are still dominant (53.7 %), despite the weight-sharing scheme. *Neurons* start to become an important factor as well (45.6 %). This is only due to the persistent neuron states. For stateless neurons, the memory requirements are weight dominated, demonstrating a high memory efficiency of our architecture also for stateless neurons and low-bit-width weight quantization.

Fig. 6 shows that the memory requirements of the first layers are dominated by *neurons* with the proposed technique (for the considered stateful neurons). Later layers are *parameter* dominated. This strongly justifies the need for a unified memory where the section sizes for *parameters* and *neurons* can be freely assigned, as done in our taped-out chip. The growing ratio of *neuron* over *parameter* requirements is explained with the structure of a typical CNN. Early layers have a larger XY resolution than later ones. Stride-2 convolutions, non-padded convolutions, and pooling layers successively reduce the width, W, and height, H, of the FMs. On the other hand, the channel count, D increases with the depth of the layer in most CNNs. Since the neuron and weight counts of a regular convolution layer are $D \cdot W \cdot H$ and $D_{src} \cdot D \cdot KW \cdot KH$, respectively, weight requirements increase and neuron requirements decrease with the layer depth.

Most layers of the *PilotNet* CNN only take a small portion of the memory of a core with our technique. Consequently, a mapping aiming at a minimized core count, showed that the proposed synapse-compression technique allows fitting the full CNN without any further optimization in as few as 3 out of the 144 cores. With the two reference techniques, the same mapping experiment shows a core-count requirement that is at least $101 \times$ higher.

5.4 State-of-the-art CNNs

The reference neuromorphic architectures do not support sophisticated CNNs. The reason is that such complex networks do not fit in the local memories due to the large synaptic memory requirements. The proposed technique overcomes this limitation through its large compression rates, as shown in the following.

We analyze the core and memory requirements for four of today's most popular CNNs: *Google's MobileNet* [9], *ResNet50* [1], *Darknet53* [25], and *ResNet101* [1]. The first network is designed to run on mobile devices and is thus more lightweight than the other three designed for less

Table 3
Mapping of state-of-the-art CNNs with the proposed synapse-compression scheme versus prior art (in brackets the compression rates of the proposed scheme compared to prior art).

CNN	Syn. Compr.	Mem. Total	Neurons	Connectivity	Parameters
PilotNet [10]	This Work	0.45 MB	0.20 MB	3.16 kB	0.24 MB
	LUT	0.11 GB $(262\times)$	0.20 MB $(1\times)$	91.44 MB $(29.6k\times)$	25.63 MB $(107\times)$
	Hier. LUT	74.30 MB $(166\times)$	0.20 MB $(1\times)$	48.46 MB $(15.6k\times)$	25.63 MB $(107\times)$
MobileNet [9]	This Work	11.23 MB	8.00 MB	0.16 MB	3.07 MB
	LUT	1.85 GB $(169\times)$	8.00 MB $(1\times)$	1.38 GB $(8.9k\times)$	0.46 GB $(154\times)$
	Hier. LUT	1.34 GB $(123\times)$	8.00 MB $(1\times)$	0.88 GB $(5.7k\times)$	0.46 GB $(154\times)$
ResNet50 [1]	This Work	43.48 MB	17.71 MB	1.31 MB	24.45 MB
	LUT	14.60 GB $(344\times)$	17.71 MB $(1\times)$	11.03 GB $(8.6k\times)$	3.54 GB $(149\times)$
	Hier. LUT	10.26 GB $(242\times)$	17.71 MB $(1\times)$	6.70 GB $(5.2k\times)$	3.54 GB $(149\times)$
DarkNet53 [25]	This Work	51.21 MB	21.19 MB	1.36 MB	28.66 MB
	LUT	25.13 GB $(502\times)$	21.19 MB $(1\times)$	18.63 GB $(14.0k\times)$	6.48 GB $(231\times)$
	Hier. LUT	18.68 GB $(374\times)$	21.19 MB $(1\times)$	12.18 GB $(9.2k\times)$	6.48 GB $(231\times)$
ResNet101 [1]	This Work	72.23 MB	27.47 MB	2.18 MB	42.57 MB
	LUT	28.02 GB $(397\times)$	27.47 MB $(1\times)$	20.98 GB $(9.8k\times)$	7.01 GB $(169\times)$
	Hier. LUT	20.25 GB $(287\times)$	27.47 MB $(1\times)$	13.21 GB $(6.2k\times)$	7.01 GB $(169\times)$

constrained devices such as GPUs. Hence, *MobileNet* has far fewer neurons and synapses than the other three analyzed CNNs (but still many more than *PilotNet*). In particular, *ResNet101* is an extremely complex network, while *ResNet50* and *Darknet53* lay somewhere in the middle. We investigate these CNNs to quantify the gains of the proposed technique for a broad range of CNNs. Also, we show that the proposed compression technique enables the execution of even complex CNNs in a single self-contained chip. The experimental setup here is the same as for the *PilotNet* analysis in the previous subsection.

Table 3 includes the results for all analyzed networks. The results show that, with the previously published techniques, mapping CNNs more complex than *PilotNet* is out of reach. For each network, the memory requirements for *connectivity* is already far above the reasonable on-chip memory limit. This changes with the proposed technique, which compresses the memory requirements for *connectivity* compared to the best reference technique by up to 15k $\times$. In

fact, for all networks, the *connectivity* requirements become negligibly small. Even for the complex *ResNet101* CNN, only 2.18 MB are required for *connectivity*. This is far below the on-chip memory limit of modern embedded systems. Thus, in combination with other supported compression techniques such as weight pruning, low bit-width quantization, and stateless execution, even *ResNet101* is mappable for our architecture.

Due to the nature of the experimental setup, *parameters* and *neurons* dominate after applying the proposed synapse compression technique. Still, our weight-sharing approach enables us to bring the *parameter* requirements down by up to $231 \times$.

Despite the pessimistic experimental setup, our technique achieves overall memory compression rates in the range from $123 \times$ to $374 \times$ compared to the published state-of-the-art. Another advantage of the proposed technique is that it has larger gains for complex networks. The memory compression rate for the lightweight CNNs *MobileNet* and *Pilotnet* are the lowest. For the complex CNNs *Darknet53* and *ResNet101*—for which a high compression rate is crucial—the overall compression is about $300 \times$.

The reason is that complex CNN layers have much more channels, resulting in many more synapses per neuron. With an increasing synapse count per neuron, the compression rate of the proposed technique grows, as our technique only requires one axon to describe the connectivity between two neuron populations, irrespective of the synapse count in between. This increases the mappability of complex CNNs on our event-based architecture.

Finally, we want to draw again an abstract comparison with *Loihi 2*, for which the technology brief reports a synapse compression of up to $17\times$ for CNNs without disclosing the technique fully [2]. Compared to the stated $17\times$ best-case reduction by *Loihi2*, we achieve another factor of at least $18 \times$ (*PilotNet*) and up to $37 \times$ (*DarkNet53*) on top. This demonstrates the clear advantage of the proposed technique over not only the published state-of-the-art but also over upcoming commercial architectures.

6 CONCLUSION

This work presents a technique to compress the synaptic memory in neuromorphic event-based massive-multicore architectures for efficient CNN inference. The technique is based on two lightweight hardware blocks substituting memory costly look-up tables. Our proposed technique has been taped-out in a 144-core event-based CNN accelerator using a 12-nm technology. The hardware overhead of the proposed technique was found to be negligible. Nevertheless, it demonstrates compression rates for various modern CNNs ranging from $123\times$ to $374\times$.

A systematic combination of the proposed technique with *orthogonal* weight and neuron compression schemes is left for future work. With such techniques, we will be even able to run extremely complex CNNs on a small form-factor chip in a temporal-sparse event-based fashion at low power consumption, latency, and cost.

REFERENCES

[1] K. He, X. Zhang, S. Ren, and J. Sun, "Deep residual learning for image recognition," in *Proceedings of the IEEE conference on computer vision and pattern recognition*, 2016, pp. 770–778.

[2] "Taking neuromorphic computing with Loihi 2 to the next level – Technology Brief," https://download.intel.com/newsroom/2021/new-technologies/neuromorphic-computing-loihi-2-brief.pdf, (Accessed on 10/21/2021).

[3] O. Moreira, A. Yousefzadeh, F. Chersi, A. Kapoor, R.-J. Zwartenkot, P. Qiao, G. Cinserin, M. A. Khoei, M. Lindwer, and J. Tapson, "Neuronflow: A hybrid neuromorphic–dataflow processor architecture for AI workloads," in *2020 2nd IEEE International Conference on Artificial Intelligence Circuits and Systems (AICAS)*. IEEE, 2020, pp. 01–05.

[4] F. Akopyan, J. Sawada, A. Cassidy, R. Alvarez-Icaza, J. Arthur, P. Merolla, N. Imam, Y. Nakamura, P. Datta, G.-J. Nam *et al.*, "Truenorth: Design and tool flow of a 65 mW 1 million neuron programmable neurosynaptic chip," *IEEE transactions on computer-aided design of integrated circuits and systems*, vol. 34, no. 10, pp. 1537–1557, 2015.

[5] P. O'Connor and M. Welling, "Sigma delta quantized networks," *arXiv preprint arXiv:1611.02024*, 2016.

[6] S. Moradi, N. Qiao, F. Stefanini, and G. Indiveri, "A scalable multicore architecture with heterogeneous memory structures for dynamic neuromorphic asynchronous processors (DYNAPs)," *IEEE transactions on biomedical circuits and systems*, vol. 12, no. 1, pp. 106–122, 2017.

[7] S. B. Furber, F. Galluppi, S. Temple, and L. A. Plana, "The SpiNNaker project," *Proceedings of the IEEE*, vol. 102, no. 5, pp. 652–665, 2014.

[8] M. Davies, N. Srinivasa, T.-H. Lin, G. Chinya, Y. Cao, S. H. Choday, G. Dimou, P. Joshi, N. Imam, S. Jain *et al.*, "Loihi: A neuromorphic manycore processor with on-chip learning," *IEEE Micro*, vol. 38, no. 1, pp. 82–99, 2018.

[9] A. G. Howard, M. Zhu, B. Chen, D. Kalenichenko, W. Wang, T. Weyand, M. Andreetto, and H. Adam, "MobileNets: Efficient convolutional neural networks for mobile vision applications," *arXiv preprint arXiv:1704.04861*, 2017.

[10] M. Bojarski, D. Del Testa, D. Dworakowski, B. Firner, B. Flepp, P. Goyal, L. D. Jackel, M. Monfort, U. Muller, J. Zhang *et al.*, "End to end learning for self-driving cars," *arXiv preprint arXiv:1604.07316*, 2016.

[11] "BrainChip," https://brainchip.com/, (Accessed on 11/03/2022).

[12] S. Han, H. Mao, and W. J. Dally, "Deep compression: Compressing deep neural networks with pruning, trained quantization and Huffman coding," *arXiv preprint arXiv:1510.00149*, 2015.

[13] S. Xie, R. Girshick, P. Dollár, Z. Tu, and K. He, "Aggregated residual transformations for deep neural networks," in *Proceedings of the IEEE conference on computer vision and pattern recognition*, 2017, pp. 1492–1500.

[14] B. Jacob, S. Kligys, B. Chen, M. Zhu, M. Tang, A. Howard, H. Adam, and D. Kalenichenko, "Quantization and training of neural networks for efficient integer-arithmetic-only inference," in *Proceedings of the IEEE conference on computer vision and pattern recognition*, 2018, pp. 2704–2713.

[15] M. Rastegari, V. Ordonez, J. Redmon, and A. Farhadi, "XNOR-net: Imagenet classification using binary convolutional neural networks," in *European conference on computer vision*. Springer, 2016, pp. 525–542.

[16] T. Serrano-Gotarredona, B. Linares-Barranco, F. Galluppi, L. Plana, and S. Furber, "ConvNets experiments on SpiNNaker," in *2015 IEEE International Symposium on Circuits and Systems (ISCAS)*. IEEE, 2015, pp. 2405–2408.

[17] A. Zhang, Z. C. Lipton, M. Li, and A. J. Smola, "Dive into deep learning," *arXiv preprint arXiv:2106.11342*, 2021.

[18] A. Aimar, H. Mostafa, E. Calabrese, A. Rios-Navarro, R. Tapiador-Morales, I.-A. Lungu, M. B. Milde, F. Corradi, A. Linares-Barranco, S.-C. Liu *et al.*, "NullHop: A flexible convolutional neural network accelerator based on sparse representations of feature maps," *IEEE transactions on neural networks and learning systems*, vol. 30, no. 3, pp. 644–656, 2018.

[19] Z. Zhu, A. Pourtaherian, L. Waeijen, L. Bamberg, E. Bondarev, and O. Moreira, "ARTS: An adaptive regularization training schedule for activation sparsity exploration," in *2022 25th Euromicro Conference on Digital System Design (DSD)*. IEEE, 2022, pp. 415–422.

[20] Y. Cao, Y. Chen, and D. Khosla, "Spiking deep convolutional neural networks for energy-efficient object recognition," *International Journal of Computer Vision*, vol. 113, no. 1, pp. 54–66, 2015.

[21] O. Ronneberger, P. Fischer, and T. Brox, "U-net: Convolutional networks for biomedical image segmentation," in *International Conference on Medical image computing and computer-assisted intervention*. Springer, 2015, pp. 234–241.

[22] S. Han, X. Liu, H. Mao, J. Pu, A. Pedram, M. A. Horowitz, and W. J. Dally, "EIE: Efficient inference engine on compressed deep neural network," *ACM SIGARCH Computer Architecture News*, vol. 44, no. 3, pp. 243–254, 2016.

[23] T. Tambe, E.-Y. Yang, Z. Wan, Y. Deng, V. J. Reddi, A. Rush, D. Brooks, and G.-Y. Wei, "Adaptivfloat: A floating-point based data type for resilient deep learning inference," *arXiv preprint arXiv:1909.13271*, 2019.

[24] Y. He, X. Zhang, and J. Sun, "Channel pruning for accelerating very deep neural networks," in *Proceedings of the IEEE international conference on computer vision*, 2017, pp. 1389–1397.

[25] J. Redmon and A. Farhadi, "Yolov3: An incremental improvement," *arXiv preprint arXiv:1804.02767*, 2018.

BIOGRAPHIES

Luc Waeijen received the B.Sc., M.Sc., and Ph.D. degrees from the Eindhoven University of Technology (TU/e), in 2012, 2013, and 2022, respectively. He is a Senior Computer Architect at GrAI Matter Labs, driving the design and specification of neuromorphic processors.

Anupam Chahar received the B.Sc. from Jaypee University of Information Technology in 2010 and the M.Sc. from TU Delft in 2012. Since 2022, he is a Lead Cryptography Firmware Engineer at PQshield. In the past, he held various software engineering positions at ASML, Intrinsic ID, Intel, and GrAI Matter Labs.

Lennart Bamberg received the B.Sc., M.Sc., and Ph.D. degree with *summa cum laude* in electrical and information engineering from the University of Bremen, Germany, in 2014, 2016, and 2020 respectively. He has been a Research Scholar at Georgia Tech and a Technical Director at GrAI Matter Labs. Currently, he is a Principal Architect at NXP where he is responsible for the company's AI IPs. Moreover, he is a lecturer at the University of Bremen.

Orlando Moreira received a Ph.D. degree in electrical engineering from the Technical University of Eindhoven, The Netherlands, in 2012. He has been a Research Scientist with Philips Research, a Senior Scientist with NXP Semiconductors, and a Principal Engineer with ST-Ericsson and Intel. He is currently Chief Architect at GrAI Matter Labs, where he is also responsible for the compute architecture.

Arash Pourtaherian received the B.Sc. degree in electrical engineering jointly from Indiana University–Purdue University, Indianapolis, IN, USA, and the University of Tehran, Iran. In 2010 and 2018 respectively he received the M.Sc. and Ph.D. degree in electrical engineering from the Eindhoven University of Technology. From 2018 to 2019 he was a post-doc at the Eindhoven University of Technology. Currently, he is a Principal Computer Architect at GrAI Matter Labs.